Dimer integrable systems

Vautouraude - Oct. 2019

Valdo Tatitscheff

valdo.tatitscheff@math.unistra.fr

IRMA, 7 rue René Descartes, 67084 Strasbourg Cedex

October 24, 2019

Abstract

Hey Hey Hey [GK13]

Contents

1 What is integrability ? 1
- 1.1 Phase spaces, integrals of motion and Arnold-Liouville theorem . . . 1
- 1.2 Quantum integrable systems . . . 3
- 1.3 Algebraic integrable systems . . . 6

2 Dimer integrable systems 6
- 2.1 Bipartite graphs and weight functions . . . 6
- 2.2 Kasteleyn matrices and partition functions . . . 6
- 2.3 The dimer model as a gauge theory on Γ . . . 8
- 2.4 Bipartite fat graphs . . . 9
- 2.5 Poisson structures . . . 10
- 2.6 Local definition of the Poisson structure . . . 11

3 Bipartite fat graphs on $\mathbb{T}^2$: cluster structure and integrability 12
- 3.1 The cluster nature of the dimer model . . . 12
- 3.2 Casimirs . . . 14
- 3.3 Hamiltonians and integrability . . . 15
  - 3.3.1 The Hamiltonians Poisson-commute . . . 15
  - 3.3.2 Counting the Hamiltonians . . . 17
  - 3.3.3 Spectral curves and the linear independence of the Hamiltonians . . . 17
- 3.4 An explicit example . . . 18

4 Concluding remarks 19
- 4.1 Two follow-up bounces . . . 19
  - 4.1.1 A generalisation to other Lie groups . . . 19
  - 4.1.2 The inverse spectral problem . . . 19
- 4.2 AdS/CFT correspondence, brane tilings and mirror symmetry . . . 20
- 4.3 A conjectural quantization condition through topological strings . . . 21

1 What is integrability ?

1.1 Phase spaces, integrals of motion and Arnold-Liouville theorem

Newton's second law In this section we aim at the (mathematical) description of classical, non-relativistic (physical) systems with finitely many degrees of freedom. Very often, such a dynamics can be described by Newton's second law. There are other formalisms that are more general (in some sense), and more convenient (in some cases). We will come back to them in a short while. For now, let us restrict to a simple, non-generic case in order to fix the ideas.

Assume that the system under consideration has n *generalized coordinates*, say $(q^1, ..., q^n) \in \mathbb{R}^n$ (as are the two coordinates needed to describe the position of a point with a mass moving on a place), to which are associated n *generalized momenta* $(p_1, ..., p_n)$ (as are the two coordinates of the speed of that point). The total space $\mathcal{M} = \{q^1, ..., q^n, p_1, ..., p_n\} \simeq \mathbb{R}^{2n}$ is called *phase space* of the system. An evolution of the latter is a trajectory in phase space, parametrised by *time*: the positions and speed coordinates evolve in an intricate way.

Newton's second law describes the *physical* evolution of the system. Let $\gamma : [-T_0, T_0] \to M$ be any trajectory in phase space. Then Newton's second law says it is physical if

$$\frac{d}{dt} p_k(\gamma(t)) = F_i(q_i, p_j, ...)$$

holds for every $i \in [1, .., n]$, for some functions F_i called *forces*.

The lesson here is that a classical mechanical system exhibits a structure of phase space (which somehow contains the information of how coordinates relate to momenta), and then some choices (as the forces) define a special *physical* evolution of the system, following general principles.

There are two major generalisations of Newton's second law called Lagrange's and Hamilton's formalisms. We are especially interested in the second one, hence we will spend no time on the first nor any more time on Newton's formalism, and refer to [Arn89] for more on these.

Hamiltonian description of dynamics In Hamilton description of mechanics, the relationship between coordinates and momenta is given by a Poisson bracket on phase space, whereas the dynamics is induced from the choice of a *Hamiltonian function*, or Hamiltonian. The Poisson bracket on the phase space $\mathcal{M} = (q^1, ..., q^n, p^1, ..., p^n)$ of above is the following map:

$$\begin{array}{rcl} \mathcal{C}^\infty(\mathcal{M}) \times \mathcal{C}^\infty(\mathcal{M}) & \to & \mathcal{C}^\infty(\mathcal{M}) \\ (f, g) & \mapsto & \displaystyle\sum_{i,j=1}^{n} \frac{\partial f}{\partial q_i}\frac{\partial g}{\partial p_j} - \frac{\partial f}{\partial p_i}\frac{\partial g}{\partial q_j} \end{array}$$

Properties 1. *One can see that for all i and j:*

- $\{q_i, q_j\} = \{p_i, p_j\} = 0$
- $\{q_i, p_j\} = \delta_{ij}$

The Poisson bracket is bilinear, antisymmetric, and it satisfies Leibniz's identity in each of its entries, that is, for $f, g, h \in \mathcal{C}^\infty(\mathcal{M})$:

$$\{fg, h\} = f\{g, h\} + g\{f, h\};\ \{f, gh\} = g\{f, h\} + h\{f, g\} \tag{1}$$

A consequence of that is that the choice of a Poisson bracket $\{\}$ is equivalent to the data of a bivector field *$\pi \in \Gamma(\bigwedge^2 T\mathcal{M})$ such that $\{f, g\} = \pi(df \wedge dg)$.*

A Hamiltonian is a function $H \in \mathcal{C}^\infty(\mathcal{M})$. A trajectory in phase space $\gamma : I \to \mathcal{M}$ (where I is in time interval) is physical if it satisfies Hamilton's equations:

$$\frac{d}{dt} q_i(\gamma(t)) = \{H, q_i(\gamma(t))\}, \text{ and } \frac{d}{dt} p_i(\gamma(t)) = \{H, p_i(\gamma(t))\}\ .$$

Omitting from now on the γ and referring to trajectories in phase-space simply as $(q_1(t), ..., q_n(t), p_1(t), ..., p_n(t))$, these equations read:

$$\frac{d}{dt} q_i(t) = \{H, q_i(t)\}, \text{ and } \frac{d}{dt} p_i(t) = \{H, p_i(t)\}\ . \tag{2}$$

In fact, thanks to Leibniz identity, the time evolution of any function $f \in \mathcal{C}^\infty(M)$ is given by:

$$\frac{d}{dt} f(q_1(t), ..., q_n(t), p_1(t), ..., p_n(t)) = \{H, f(q_1(t), ..., q_n(t), p_1(t), ..., p_n(t))\}\ , \tag{3}$$

written, for short, as:

$$\frac{d}{dt} f = \{H, f\}\ . \tag{4}$$

Remark 1. *The Hamiltonian function H defines a vector field $\pi(dH, \cdot)$ on $\mathcal{M}$. A trajectory $\gamma : I \to \mathcal{M}$ is physical if the restriction of $\pi(dH, \cdot)$ to $\gamma(I)$ the image of γ coincides with the push-forward of the forward unit tangent vector on I.*

Examples 1. *1. The classical harmonic oscillator of mass $m > 0$ and tension $k > 0$ has a two-dimensional phase space parametrized by (q, p), with Hamiltonian:*

$$H = \frac{p^2}{2m} + k\frac{x^2}{2}\ .$$

2. A particle of mass m evolving in $\mathbb{R}^3$, in the gravitational field *of a planet of mass M placed at the origin $0 \in \mathbb{R}^3$, form a physical system with a six-dimensional phase space, parametrised with three coordinates (q_1, q_2, q_3) and three associated momenta (p_1, p_2, p_3). The Hamiltonian is given by:*

$$H = \sum_i \frac{p_i^2}{2m} - \frac{\mathcal{G}Mm}{\sqrt{\sum_i x_i^2}}\ .$$

Poisson manifolds A natural generalisation of the systems presented above, is to take as a definition of a physical system a Poisson manifold together with a Hamiltonian function.

Definition 1. *A Poisson bracket on a manifold $\mathcal{M}$ is an antisymmetric bilinear map $\mathcal{C}^\infty(\mathcal{M}) \times \mathcal{C}^\infty(\mathcal{M}) \to \mathcal{C}^\infty(\mathcal{M})$ that satisfies the Leibniz identity is each of its entries, together with the Jacobi identity:*

$$\{f, \{g, h\}\} + \{g, \{h, f\}\} + \{h, \{f, g\}\} = 0 \ . \tag{5}$$

A Poisson manifold is a manifold endowed with a Poisson bracket.

A Poisson bracket is said to be degenerate if there is a function $f \in \mathcal{C}^\infty(\mathcal{M})$ such that for every other $g \in \mathcal{C}^\infty(\mathcal{M})$, one has $\{f, g\} = 0$. Such a function f is called a Casimir of the Poisson bracket. Whenever a Poisson bracket is degenerate, fixing the value of one of its Casimir, and restricting oneself to the corresponding level hypersurface of this Casimir in phase space yields a *less-degenerate* Poisson bracket. Doing that procedure again and again enough times yield in the end a Poisson bracket which is non-degenerate. It is a fact that the corresponding submanifolds (the ones one gets by fixing the value of a maximal collection of Casimirs) are even dimensional. Half this dimension is called the *rank* of the Poisson bracket.

Integrals of motion

Definition 2. *A integral of motion of a dynamical system is a quantity that is constant along the evolution of the system. In the Poisson framework, Eq.* 4 *implies that an integral of motion can equivalently be defined as a function $f \in \mathcal{C}^\infty(\mathcal{M})$ that commutes with the Hamiltonian, for the Poisson bracket:*

$$\{H, f\} = 0 \ . \tag{6}$$

Let $f \in \mathcal{C}^\infty(\mathcal{M})$ be some integral of motion. By definition, the physical trajectories in phase space is constrained to live on the level hypersurfaces of f, hence knowing integral of motion makes it easier to find solutions of the equations of motion. Note that an integral of motion f also defines a flow in $\mathcal{M}$ via $\{f, \cdot\}$.

Liouville integrability The case of Liouville integrability is an extreme case in the sense that there is enough integral of motions to make the dynamics trivial. Maybe after fixing the value of Casimirs, one can assume that the Poisson bracket is non-degenerate.

Definition 3. *A Hamiltonian system $(\mathcal{M}, \{\cdot, \cdot\}, H)$ with non-degenerate Poisson bracket of rank n (which implies that $\dim \mathcal{M} = 2n$) is said to be (Liouville) integrable if it has n independent, everywhere differentiable integrals of motion F_k, $k = 1..n$, that are in involution for the Poisson bracket.*

A consequence of this very strong property is that this dynamical system is *solvable by quadratures*: instead of having to solve the differential equations which are the equations of motion, one only has to solve a finite number of algebraic equations, integrals...

Remark 2. *Note that the Hamiltonian is an obvious integral of motion, and hence can be denoted F_1. As such, there is no difference at all between this F_1 and the other F_k's: for each k, the integral of motion F_k defines a flow $\{F_k, \cdot\}$, and the parameter along it is an analogue of the time for the physical evolution with Hamiltonian F_1. We can even call it the k-th time function T_k.*

The following result, known as the Arnold-Liouville theorem, expresses how constraining the framework of above is. We state it without proof, and again refer to [Arn89] for more details and a proof.

Theorem 1. *Let $(\mathcal{M}, \{\cdot, \cdot\}, H)$ be a Hamiltonian system with non-degenerate Poisson bracket of rank n, which is integrable* à la Liouville*. Evolutions in phase space are restricted to common level submanifolds of $F_1, ..., F_n$. If such a manifold is compact, then it is diffeomorphic to the n-dimensional real torus T^n.*

It is even doable to find a good system of coordinates, called action-angle coordinates, in which evolution in phase space is as simple as possible.

1.2 Quantum integrable systems

In this subsection we follow the introduction to quantization given in [CKTB05], to which we also refer for more details on that matter.

Upon quantification of a classical Hamiltonian system, one expects to replace the commutative algebra $\mathcal{C}^\infty(\mathcal{M})$ of functions on $\mathcal{M}$ with the non-commutative algebra of endomorphisms of some Hilbert space which is the *space of states* of the corresponding quantum system. Hermitian operators on this Hilbert space correspond to observables, and the rays in the Hilbert space to states of the system.

The quantum description of a system depend on a parameter $\hbar$ which is called the Planck constant. As $\hbar$ goes to zero, one expects to retrieve the classical description of the same system, and in this sense the quantum description is always more precise than the classical one.

Whereas going from the quantum description to the classical one more or less correspond to taking some kind of limit, going in the opposite direction is by far less obvious. There have been two main approaches:

- Geometric quantization
- Deformation quantization

In order to understand the differences between the two different quantization frameworks, let's first consider the easy example of a topologically trivial classical phase space $\mathcal{M} = \mathbb{R}^{2n}$, with coordinates $q_1, ..., q_n, p_1, ..., p_n$ - for example, corresponding to a massive particle moving in a n-dimensional potential $V \in \mathcal{C}^\infty(\mathbb{R}^n)$, in which case the classical Hamiltonian is:

$$H(q_1, ..., q_n, p_1, ..., p_n) = \sum_{i=1}^{n} \frac{p_i^2}{2} + V(q_1, ..., q_n) \ . \tag{7}$$

The Poisson bracket is the canonical one, given in Properties 1. The corresponding quantized system is the data of the Hilbert space of square-integrable functions in the variables $q_1, ..., q_n$:

$$\mathcal{H} = \mathbb{L}^2(\mathbb{R}^n) \ , \tag{8}$$

on which the quantum equivalent of the classical functions q_i and p_i act as operators, and are given by:

$$Q_i\psi(q_1, ..., q_n) = q_i\psi(q_1, ..., q_n) \text{ and } P_i\psi(q_1, ..., q_n) = -i\hbar\frac{\partial}{\partial q_i}\psi(q_1, ..., q_n) \tag{9}$$

and where the classical Poisson bracket has been *replaced* by the following quantum commutator:

$$[Q_i, P_j] = i\hbar\delta_{ij}, \ [Q_i, Q_j] = [P_i, P_j] = 0 \ . \tag{10}$$

The quantum Hamiltonian is the hermitian operator on $\mathcal{H}$ defined by:

$$\hat{H} = \sum_{i=1}^{n} -\frac{\hbar^2}{2}\frac{\partial^2}{\partial q_i^2} + V(Q_1, ..., Q_n) \ , \tag{11}$$

and the possible energy levels of the system correspond to its eigenvalues, with their corresponding eigenstates. These eigenvalues are the possible outcomes of an energy measurement of the system. As emphasized above, the smaller $\hbar$, and the closer the eigenvalues get, so that in the limit $\hbar \to 0$ one retrieves the *classical approximation* of the quantum system.

What can go wrong in general? When the phase space of the classical system does not have a trivial topology, it can happen that it is difficult to *separate* the phase space into coordinates and momenta. Locally, it can always be done, of course (thanks to Darboux's theorem), but it is by far not obvious that it can be done globally. A case where this problem does not arise, and which is more general than the example presented above, is the one where the phase space is obtained as the *cotangent bundle of a smooth manifold*, for example, when one studies the motion of a point particle living on some n-dimensional manifold. The phase space is indeed the (co-)tangent bundle of this manifold, and there is a special section of this bundle (the canonical inclusion of the manifold as the zero section) which allows to distinguish globally coordinates and momenta.

This is the case of pendula, for example: the single coordinate lives on a circle (and not on a line), and the classical phase space is the cotangent bundle of the circle, which topologically is a cylinder.

However, when the phase space is not obtained as the cotangent bundle of a coordinate manifold, it may be very difficult (or impossible) to choose some globally defined $q_1, ..., q_n$ amongst the $2n$ coordinates in order to define the Hilbert space as $\mathbb{L}^2(q_1, ..., q_n)$.

Geometric quantization In the geometric quantization setting, one explicitly construct the wanted Hilbert space, and the algebra of operators that acts on it. The method strongly relies on the symmetries of the phase space (and applies to phases spaces which are co-adjoint orbits of Lie groups - a more general case that the ones presented above). It has a mathematical avatar known as the *orbit method* in the theory of representation of Lie groups (see [CKTB05]).

I have been explained geometric quantization by V. Fock, and used these personal notes together with the Baez's blog page [Bae18] on the topic to write the following few lines.

We start from a classical phase space, i.e. a Poisson manifold, and assume the Poisson bracket to be non-degenerate, otherwise one fixes the values of its Casimirs until it is non-degenerate. A non-degenerate Poisson bracket is a bivector $\pi \in \bigwedge^2 T\mathcal{M}$ of maximal rank, and its dual is non-degenerate 2-form ω. The fact that the Poisson bracket satisfies the Jacobi identity implies that ω is closed. In other words, ω is a symplectic form, and $(\mathcal{M}, \omega)$ is a symplectic manifold.

- The first step in the construction is to chose a hermitian line bundle L over $\mathcal{M}$ with principal $U(1)$-connection Δ, so that its curvature equals $i\omega$. There is a possible obstruction to that step, which generalises Bohr-Sommerfeld quantization condition: $\omega/2\pi$ has to define an integral cohomology class. Moreover, as explain in [Bae18], the condition on the curvature fixes the bundle only partially, and there are choices to make.
- One wants to think of this hermitian line bundle as the generalization of the complex line in the examples presented above; instead of having as Hilbert space of space of complex-valued functions, the Hilbert space will be a space of sections of this hermitian line bundle. However, if one defines and chooses - naively, all the square-integrable sections of this bundle, it would be as if one had chosen as Hilbert space in the topologically trivial case *all* the square-integrable functions in $q_1, ..., q_n, p_1, ..., p_n$, and not only those that merely depend on $q_1, ..., q_n$.

- To implement this constraint, one has to separate between coordinates and momenta (and do it in a global way) and then imposes some kind of condition, like keeping only the functions that are constant *in the direction of the momenta*. This is exactly what the aim is: first one has to choose a *polarisation*, the easiest examples of which are said to be *real polarisations*, and are *integrable lagrangian distributions* on $\mathcal{M}$. This amounts to locally foliate $\mathcal{M}$ with half-dimensional submanifolds, on which the restriction of the symplectic form (or equivalently, the Poisson bracket) has to be trivial, and which glue together well globally.
- Eventually, one defined the quantum Hilbert space as the Hilbert space of square-integrable functions on M which are covariantly constant in the direction of the polarisation.

Deformation quantization Again following the introduction given in [CKTB05], we now turn to deformation quantization. Now the goal is, from a symplectic or Poisson manifold $\mathcal{M}$, to deform the (commutative) algebra of smooth functions on $\mathcal{M}$ into a (non-commutative) algebra of operators, in the following way. One defines a *deformed multiplication*, such that the product defined for $f, g \in \mathcal{C}^\infty(\mathcal{M})$:

$$f \star g = \sum_{n=0}^{\infty} B_n(f,g)t^n \ , \tag{12}$$

extends to an *associative* multiplication on the space $\mathcal{C}^\infty(M)[[t]]$ of formal series in t with coefficients smooth functions on M. Associativity is equivalent to the following identities, for $n \geq 0$:

$$\sum_{j+k=n} B_j(f, B_k(g,h)) = \sum_{j+k=n} B_j(B_k(f,g),h) \ . \tag{13}$$

If moreover the B_n are bi-differential operators (involving sums of products of f and g and their derivatives), then $\star$ is said to be a star-product.

Since $\star$ defines an associative product on $\mathcal{C}^\infty(M)[[t]]$, the bracket $[f,g] = f \star g - g \star f$ satisfies Jacobi identity and makes $\mathcal{C}^\infty(M)[[t]]$ into a Lie algebra.

Definition 4. *A deformation quantization of a Poisson manifold $(\mathcal{M}, \{\cdot,\cdot\}$ is a star-product $\star$ such that*

$$[f,g] \to \{f,g\} \ ,$$

as t goes to 0. This last condition is equivalent to

$$B_1(f,g) - B_1(g,f) = \{f,g\} \ .$$

Deformation quantization has been defined and studied for the first time in 1978 in [BFF$^+$78a] and [BFF$^+$78b], and then several results concerning deformation quantization of symplectic manifolds have been obtained by M. DeWilde, P. Lecompte and B.V. Fedosov in the first half of the 80's. In his 1997 article [Kon03], Kontsevich used a different approach to construct a globally defined star-product on an arbitrary *smooth* Poisson manifold, and proved the bijection between equivalence classes of formal deformations and equivalence classes of star-products.

Once again, we refer to [CKTB05] - the first third of the book being devoted to the presentation of Kontsevich's results, and especially chapter 2 which gives a clear overview of the construction.

Quantum integrability: the philosophy. After this aside on some mathematical ideas concerning quantization, let's now turn to some quick implications of integrability in a quantum framework.

The guiding principle of quantization is to replace the Poisson bracket by a quantum commutator:

$$\{\cdot,\cdot\} \rightsquigarrow \frac{1}{i\hbar}[\cdot,\cdot] \ . \tag{14}$$

In a classical Poisson integrable system where the Poisson bracket has rank n, one has n linearly independent and differentiable *Hamiltonians* $H_1, ..., H_n$, which are in involution for the Poisson bracket:

$$\{H_i, H_j\} = 0 \tag{15}$$

Upon quantization, one expects the classical Hamiltonians to be replaced by quantum analogues $\hat{H}_1, ..., \hat{H}_n$: hermitian operators that act on a Hilbert space (in the geometric framework). Then Eq. 15 becomes:

$$[\hat{H}_i, \hat{H}_j] = 0 \ , \tag{16}$$

and subsequently one expects these $\hat{H}_i$ to be co-diagonalisable. A natural question is a quantum integrable system is then, *what are the common eigenvalues of the quantum Hamiltonians*, where by common eigenvalue we mean the eigenvalues of the Hamiltonians in a common eigenvector hermitian basis of the Hilbert space. It is a difficult question, in general.

Another point of view on the same idea is the following. According to Arnold-Liouville theorem, assuming that the level sets of the classical Hamiltonians are all compact, the structure of phase space is a torus fibration over a base which parametrizes the values of the Hamiltonians. The coordinates on the tori are the angle coordinates, or *times*. In the quantum framework, some discrete points in the base of the fibration are preferred, or distinguished, in the sense that they are the common eigenvalues of the quantum Hamiltonians. How can one get some information about these points ?

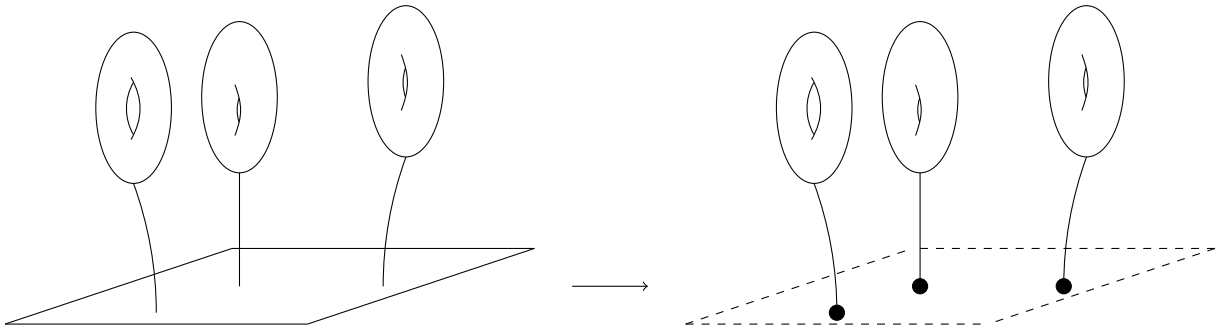

Figure 1: From classical to quantum: distinguishing points on the base.

1.3 Algebraic integrable systems

The smooth framework described above can be made more algebro-geometric: there are for example holomorphic integrable systems, in which the phase space is a complex manifold, where one considers regular functions such as holomorphic ones instead of smooth $\mathcal{C}^\infty$ ones, and with holomorphic Poisson brackets. Everything transfers well to this framework, there is a equivalent of the Arnold-Liouville theorem, the phase space also is the total space of a torus fibration, but this time with complex tori, and one can define deformation quantization is a completely analogous way.

2 Dimer integrable systems

2.1 Bipartite graphs and weight functions

Definition 5. *A bipartite graph Γ is a pair $(V_W \amalg V_B, E)$ such that E is a subset of $V_W \times V_B$, i.e. it is a graph with vertices of two types (say, white and black vertices) such that each edge connects a white vertex with a black one. In the following, all the bipartite graphs we consider are finite.*

Definition 6. *A dimer configuration on such a graph $\Gamma = (V_W \amalg V_B, E)$ is the data of a subset D of E, such that each vertex $v \in V_W \amalg V_B$ is the end of* exactly *one edge in D.*

Let us choose a *weight function* on the edges:

$$w : E \to \mathbb{C}^\times \ . \tag{17}$$

Such a weight function defines the *energy* $\mathcal{E}(D) \in \mathbb{C}^\times$ of a dimer configuration D, as:

$$\mathcal{E}(D) := \prod_{e \in D} w(e) \ . \tag{18}$$

2.2 Kasteleyn matrices and partition functions

It is a classical result that the dimer configurations of any bipartite graph Γ can be easily computed by looking at the determinant of its *Kasteleyn matrix*. First, one assigns signs (plus or minus) to the edges of Γ in such a way that every cycle of edges that has length a multiple of 4 (resp., is 2 modulo 4) has an odd (resp. even) number of minus signs on its edges. This is related to what's called a *Pfaffian orientations* of the graph.

Definition 7. *The Kasteleyn matrix of a bipartite graph Γ with weight function w is the weighted (by w multiplied by the signs evoked just above) adjacency matrix of Γ.*

The determinant of the Kasteleyn matrix computes all the dimer configurations of the graph Γ, in the sense that each term in this determinant is exactly the energy of a dimer configuration (together with a sign that comes from the determinant), that every dimer configuration appears exactly once in this sum, and that if the weight function is kept generic then inspection of the terms appearing in each product yields the exact composition of each dimer configuration. See Figures 2 and 3 for an example.

Definition 8. *The statistical partition function Z of the dimer model on Γ with weight function w is:*

$$Z(\Gamma, w) = \det K \tag{19}$$

If Γ is embedded in a surface Σ of genus g, we can keep track of the *relative* winding of two dimer configurations in a following way. The *difference* of two dimer configurations is an union of loops on Γ (possibly trivial), and defines a homology class in $H_1(\Sigma, \mathbb{Z})$. If a fundamental domain of the surface has been chosen, one can add $2g$ variables $x_1, ..., x_g, y_1, ..., y_g$ to our picture, and multiply the weight of each edge of Γ that goes out the chosen fundamental domain by the corresponding product of variables. Each dimer configuration is thereby assigned a monomial $x_1^{k_1} ... x_g^{k_g} y_1^{l_1} ... y_g^{l_g}$, or, equivalently, a vector $(k_1, ..., k_g, l_1, ..., l_g) \in \mathbb{Z}^{2g}$.

This assignment depend on the choice of fundamental domain. However, changing from one to another results in a global translation in $\mathbb{Z}^{2g}$. Let's again emphasize that the homology class of the difference of two dimer configurations is well-defined, but a dimer configuration does not have a homology class on its own. Something one can do is to fix a reference dimer configuration, and then define homologies of dimer configurations with respect to this one. Then one speaks on the *height* of a dimer configuration.

Example 1. *Consider the example given in Figure* 2. *Each edge of* Γ *is oriented from black to white. One (arbitrarily) chooses to multiply each edge that crosses positively the vertical boundary of the fundamental domain (oriented from bottom to top) by* x *(hence the edge between* B *and* 4 *gets multiplied by* x*), each edge that crosses negatively the same curve is multiplied by* x^{-1} *(hence the edge between* D *and* 2 *is multiplied by* x^{-1}*)), and similarly with* y *and the horizontal boundary of the fundamental domain, oriented from left to right.*

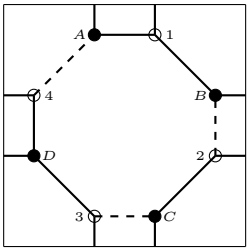

$$K := \begin{bmatrix} w_{A1} & w_{B1} & y^{-1}w_{C1} & 0 \\ 0 & -w_{B2} & w_{C2} & x^{-1}w_{D2} \\ yw_{A3} & 0 & -w_{C3} & w_{D3} \\ -w_{A4} & xw_{B4} & 0 & w_{D4} \end{bmatrix} \tag{20}$$

Figure 2: A bipartite graph on $\mathbb{T}^2$ and its Kasteleyn matrix. Dashed edges carry a -1 sign.

The adjacency matrix obtained by taking into account the weights, the procedure as the one described in Example 1 and the Pfaffian orientation of the graph is still called Kasteleyn matrix, and its determinant, the partition function of the dimer model. The difference between the latter and the former partition function is that the new one is a *Laurent polynomial* in the variables $x_1, ..., x_g, y_1, ..., y_g$.

Example 2. *For example, the partition function of the bipartite graph in Fig.* 2 *is:*

$$Z(x,y) = (w_{A1}w_{B2}w_{C3}w_{D4} + w_{B1}w_{C2}w_{D3}w_{A4} + w_{C1}w_{B2}w_{A3}w_{D4} + w_{C1}w_{D2}w_{A3}w_{B4} + w_{C1}w_{D2}w_{A3}w_{B4}) +$$
$$w_{B1}w_{C2}w_{A3}w_{D4}y + w_{C1}w_{B2}w_{D3}w_{A4}y^{-1} + w_{B1}w_{D2}w_{C3}w_{A4}x^{-1} + w_{A1}w_{C2}w_{D3}w_{B4}x \ .$$

As teased above, this determinant computes *the dimer configurations of the bipartite graph, as shown explicitly in Fig.* 3. *Each term in the partition function is the energy of a dimer configuration, together with the piece of information given by the* x *and* y *variables.*

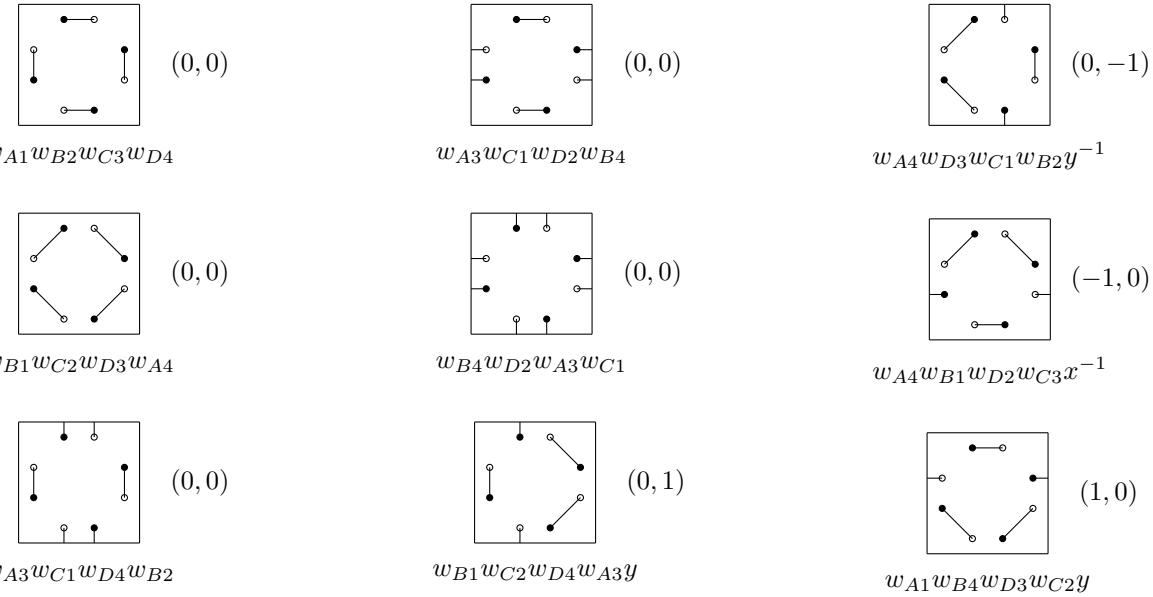

Figure 3: The nine dimer configurations of the bipartite graph shown in Fig. 2

The partition function Z (as a Laurent polynomial in $x_1, ..., x_g, y_1, ..., y_g$) defines a Newton polygon $\Delta \subset \mathbb{Z}^{2g}$ as the convex hull of the points $(k_1, ..., k_g, l_1, ..., l_g)$ corresponding to the monomials appearing in Z.

Example 3. *The monomials in the partition function given in Example* 2 *correspond to the points* $(0,0), (-1,0), (1,0), (0,-1)$ *and* $(0,1)$. *Hence the Newton polygon is the one given in Fig.* 4.

Remark 3.

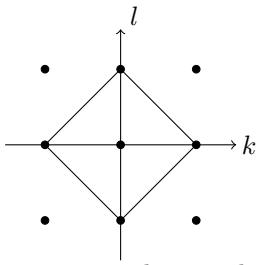

Figure 4: The Newton polygon corresponding to the partition function of Example 2.

2.3 The dimer model as a gauge theory on Γ

There is another way to slightly modify the partition function in order for it to have even nicer invariance property, through a normalization procedure.

Let $\Gamma = (V = V_B \amalg V_W, E \subset V_B \times V_W)$ be a bipartite graph, and let us fix a *reference dimer configuration* D_0. We define the D_0-normalised partition function as:

$$Z'_{D_0}(\Gamma, w, x_i, y_i) = Z(\Gamma, w, x_i, y_i)/\mathcal{E}(D_0) \ . \tag{21}$$

Does is change something in the proof of the commutation of Hamiltonians, not to normalize with a dimer configuration on the boundary of Δ but with any other one ?

Gauge invariance of the normalised partition function

Definition 9. *A gauge transformation is a function $f : V \to \mathbb{C}^\times$.*

Proposition 1. *Let f be any gauge transformation. The normalized partition function is invariant under the following change of the weights:*

$$w'(b, w) = \frac{f(w)}{f(b)} w(b, w) \tag{22}$$

for any edge (b, w) of Γ, where we have denoted w the former weight function and w' the new one.

Proof. As we have explained above, the (non-normalized) partition function is a sum:

$$\sum_D \sigma(D)\mathcal{E}(D) \ , \tag{23}$$

which runs over all dimer configurations of the graph Γ, and where $\sigma(D)$ is a sign assigned to the dimer configuration D, which depends on the choice of the Pfaffian orientation. By definition of a dimer configuration, under the transformation 22 the (non-normalized) partition gets multiplied by

$$\frac{\prod_{v_w \in V_W} v_w}{\prod_{v_b \in V_B} v_b} \ , \tag{24}$$

and the normalization $\mathcal{E}(D_0)$ by exactly the same factor, for the same reasons. Hence the transformations of the two terms cancel out, and the normalized partition function is invariant under 22. □

The transformations 22 are reminiscent of the way connections transform under gauge transformations, hence the weight function is sometimes called *discrete connection* on Γ. It is as if the vertices of Γ form the points of a 0-dimensional vector space, and the weights of the edges represent the parallel transport of an abelian $\mathbb{C}^\times$-connection. We can use this analogy to build a geometric picture, in which the gauge transformations become more natural.

Linear interpretation of the gauge transformations Instead of working with a discrete principal bundle, we are going to work with a discrete associated bundle, defined in the following way. To each vertex of Γ, we assign a complex line, together with a non-zero vector in it understood as a *basis* of the line. The weights on an edge (b, w) is understood as the single *matrix entry* of a linear map between the corresponding two complex lines L_b and L_w, in the bases given by the chosen non-zero vectors e_b and e_w respectively, as shown in Fig. 5.

A *gauge transformation* $f : V \to \mathbb{C}^\times$ is a rescaling of the basis vectors at each vertex $v \in V$: one replaces e_v with the new basis vector $f(v) \cdot e_v$. The matrix expression of the linear functions described in Fig. 5 and above it, changes as in Eq. 22.

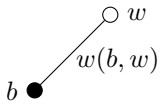

$$\begin{array}{ccc} L_b & \to & L_w \\ \alpha \cdot e_b & \mapsto & w(b,e)\alpha \cdot e_w \end{array}$$

Figure 5: Linear interpretation of the weights.

.

Moduli space of weight functions

Definition 10. *The moduli space of weight functions is the space of equivalence classes of weight functions, modulo gauge equivalence, and is denoted* $\mathcal{L}_\Gamma$.

Weight and gauge functions have a natural interpretation in terms of cellular cochains of the complex Γ: as assignments of weights to edges, the set weight functions is naturally $\mathcal{C}^1(\Gamma, \mathbb{C}^\times)$, and the gauge transformations are exactly the elements of $\mathcal{C}^0(\Gamma, \mathbb{C}^\times)$. The cellular complex of the 1-skeleton Γ is

$$0 \to \mathcal{C}^0(\Gamma, \mathbb{C}^\times) \to \mathcal{C}^1(\Gamma, \mathbb{C}^\times) \to 0 \ , \tag{25}$$

and the only non-zero map exactly corresponds to Eq. 22, in the way that a gauge transformation f naturally defines a weight function w, as $w(b, w) = f(b)^{-1} f(w)$. Hence two weight functions are gauge equivalent if and only if the are the same modulo $\mathrm{Im}\{\mathcal{C}^0(\Gamma, \mathbb{C}^\times)\}$, hence if and only if they are the same modulo coboundaries. Since the graph is merely a 1-complex, weight functions are all cocycles, and we eventually find that *the moduli space of weight functions is exactly* $H^1(\Gamma, \mathbb{C}^\times)$.

With that knowledge, how can one cleverly describe $\mathcal{L}_\Gamma$?

- There is a *conceptually useful way* which works in the case (in which we are interested) where the graph Γ is embedded in a closed, genus-g surface Σ_g, in such a way that every face, i.e. connected component of $\Sigma_g \backslash \Gamma$, is topologically a disk. Then, $H^1(\Gamma, \mathbb{C}^\times)$ is parametrized by the monodromies around all the faces of Γ but one, together with the monodromies around cycles that generate $H_1(\Sigma_g, \mathbb{Z})$. Given such cycles, it means that assigning numbers in $\mathbb{C}^\times$ to each of them and to each of the faces of $\Gamma \hookrightarrow \Sigma_g$ but one, defines a point in $\mathcal{L}_\Gamma$.
- There is also a *computationally useful way.* One merely needs to choose a spanning tree on Γ. Using exactly all the possible gauge freedom, one can fix the weight of the edges of the spanning tree to 1, and the weights of the remaining edges form a parametrization of $\mathcal{L}_\Gamma$.

2.4 Bipartite fat graphs

Fat graphs and surface graphs

Definition 11. *A* fat graph*, or ribbon graph, is a finite graph together with - a each vertex - the choice of a cyclic orientation of the incident edges.*

Let Γ be a fat graph. A face of Γ is a cycle $(\vec{e_1}, ..., \vec{e_n})$ of oriented edges of Γ recursively defined such that e_{i+1} is the edge just after e_i with respect to the cyclic orientation at the sink of $\vec{e_i}$, and the orientation of e_{i+1} is such that the source of $e_{\vec{i+1}}$ is the sink of $\vec{e_i}$. If one glues a topological disk to each face of Γ, following the orientation of the face, one obtains a oriented closed surface Σ with an inclusion $\Gamma \hookrightarrow \Sigma$.

Conversely, given an inclusion $\Gamma \hookrightarrow \Sigma$ of a graph into an orientable closed surface such that the faces are topological disks, the orientation of the surface induces a fat structure on Γ. These two notions are thus completely equivalent, and subsequently, a fat graph can be assigned a genus.

Bipartite fat graphs and dessins d'enfants In what follows, we are sometimes going to use a very useful description of bipartite fat graphs, which comes from Grothendieck's theory of dessins d'enfants: [Gro13]. See [JW16] for a complete introduction to that rich topic. Let's discuss quickly this algebraic definition of bipartite fat graphs.

First, one chooses a labelling of the edges of Γ (which we assumed finite): $E \simeq [|1, n|]$. Let x (resp. y) be the permutation of $[|1, n|]$ that sends each edge to the next one with respect to its white end (resp. black end), and let G be the subgroup of $\mathfrak{S}_n$ generated by x and y. One calls G the monodromy, or *cartographic group.* Since Γ is connected, G acts transitively on Γ.

Definition 12. *A quadruple* (G, x, y, E) *where* E *is a finite set,* x *and* y *are two permutations of* E*, and* $G = \langle x, y \rangle$ *acts transitively on* E*, is called a dessin d'enfant.*

To a dessin d'enfant, one can associate a bipartite fat graph as follows. Write the permutations x and y as a product of disjoint cycles, and let V_W (resp. V_B) be the set of cycles of y (resp. x). For each element that a cycle in V_W and a cycle in V_B have in common, add an edge between these two vertices, and label this edge with the corresponding element in E. There is a cyclic orientation of the edges incident to any vertex, induced by the orientation of the cycles in x and y.

Remark 4. *As one can easily convince oneself, the faces of the bipartite fat graph are in one-to-one correspondence with the cycles of the permutation* xy.

Fig. 6 shows the topological description (that we already know) of the bipartite fat graph in Fig. 2, where the fat structure is the one induced by the counter-clockwise orientation on the torus, together with the algebraic description as a dessin d'enfant.

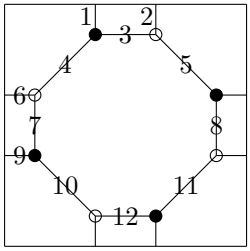

(Counterclockwisely orientated torus)

$$G = \langle x, y \rangle < \mathfrak{S}_{12}$$

$$x = (2\ 3\ 5)(4\ 6\ 7)(8\ 11\ 9)(10\ 1\ 12)$$

$$y = (1\ 4\ 3)(5\ 8\ 6)(9\ 10\ 7)(12\ 2\ 11)$$

$$E = [|1, 12|]$$

$$xy = (1\ 6\ 2\ 9)(3\ 12)(4\ 5\ 11\ 10)(7\ 8)$$

Figure 6: Topological and algebraic descriptions of the bipartite fat graph of Fig. 2

2.5 Poisson structures

Intersection pairing and Poisson structures The space of homology classes of (oriented) loops on an oriented surface Σ carries an *intersection form*, also called intersection pairing, from which one can derive interesting Poisson brackets. Two smooth loops intersecting transversally can be assigned an intersection number, which is a possibly negative integer. It counts the number of intersection of the two loops, *with sign*: since the surface is oriented, an intersection can be *positive* or *negative*, and the total number is a sum of $+1$ or -1, one for each intersection. Because each local contribution is antisymmetric in its factors, the intersection pairing is also antisymmetric. It is a fact that it is well-defined on homology classes of loops on the surface, and define an antisymmetric bilinear form in $H_1(\Sigma, \mathbb{Z})$. We will denote it

$$\epsilon : H_1(\Sigma, \mathbb{Z}) \wedge H_1(\Sigma, \mathbb{Z}) \to \mathbb{Z} \ . \tag{26}$$

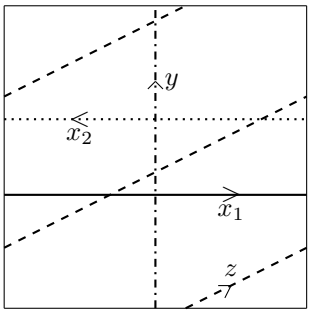

(Counterclockwisely orientated torus)

$$\epsilon(x_1, x_2) = -\epsilon(x_2, x_1) = 0$$
$$\epsilon(x_1, y) = -\epsilon(y, x_1) = +1$$
$$\epsilon(x_2, y) = -\epsilon(y, x_2) = -1$$
$$\epsilon(x_2 + z, y) = \epsilon(x_2, y) + \epsilon(z, y) = -1 + 1 = 0$$

Figure 7: Some examples of the intersection pairing on $H_1(T^2, \mathbb{Z})$.

One can define a (holomorphic) Poisson bracket on $\mathcal{L}_\Gamma$ by specifying it on the coordinate functions on $\mathcal{L}_\Gamma$, and then extend it using linearity and Leibniz rule.

Since $\mathcal{L}_\Gamma = H^1(\Gamma, \mathbb{C}^\times) = \mathrm{Hom}(H_1(\Sigma, \mathbb{Z}), \mathbb{C}^\times)$, coordinate functions on $\mathcal{L}_\Gamma$ are the monodromies along some loops that generate $H_1(\Gamma, \mathbb{Z})$. Let $W_L \in H^1(\Sigma, \mathbb{C}^\times)$ be the monodromy along the loop $L \in H_1(\Sigma, \mathbb{Z})$. It is a function:

$$W_L : \mathcal{L}_\Gamma \to \mathbb{C}^\times \ . \tag{27}$$

which associates, to each equivalence class of weight function in $\mathcal{L}_\Gamma$, the monodromy of the latter along L. To be very explicit, write:

$$L = ((b_1, \vec{w_1}), (w_1, \vec{b_2}), (b_2, \vec{w_2}), ..., (b_n, \vec{w_n}), (w_n, \vec{b_1})) \tag{28}$$

and chose a representative w of some class $[w] \in \mathcal{L}_\Gamma$. Then

$$W_L([w]) = \frac{w(b_1, w_1)w(b_2, w_2)...w(b_n, w_n)}{w(b_2, w_1)...w(b_n, w_{n-1})w(b_1, w_n)} \ . \tag{29}$$

The value of W_L does not depend on the particular representative w of $[w]$ since a gauge transformation amounts to the same factor in the numerator and the denominator of 29.

Now we use the fact that we have an embedding of Γ in the surface Σ, as follows. A loop in Γ, i.e. an element of $H_1(\Gamma, \mathbb{Z})$ defines a loop in Σ (thanks to the inclusion), i.e. an element of $H_1(\Sigma, \mathbb{Z})$, on which there is an intersection pairing. Hence it makes sense to define the Poisson bracket as:

$$\{W_{L_1}, W_{L_2}\} = \epsilon(L_1, L_2) W_{L_1} W_{L_2} \ . \tag{30}$$

Global definition of the Poisson structure on $\mathcal{L}_\Gamma$ Let $\Gamma \hookrightarrow \Sigma$ be the embedding of a bipartite graph in a torus in such a way that the faces are topological disks. The interesting Poisson structure on $\mathcal{L}_\Gamma$ (we will see later why it's interesting) is not the one induced by the intersection pairing on $H_1(\Sigma, \mathbb{Z})$ but a *twisted one*, induced by the intersection pairing on $H_1(T^2, \tilde{\Sigma}_\Gamma)$, with $\tilde{\Sigma}_\Gamma$ a conjugate surface obtained from the bipartite fat graph $\Gamma \hookrightarrow T^2$.

One starts with the bipartite fat graph Γ and reverts the cyclic orientation *at each white vertex*. Then one glues 2-cells along the faces of this new bipartite fat graph, and the resulting closed surface is $\tilde{\Sigma}_\Gamma$. In Fig. 8, we present this procedure for the embedding of Fig. 2. One should note that even if in this case $\tilde{\Sigma}_\Gamma$ is also a 2-torus, in general the genus of $\tilde{\Sigma}_\Gamma$ can be anything, and does not need to correspond to the genus of Σ.

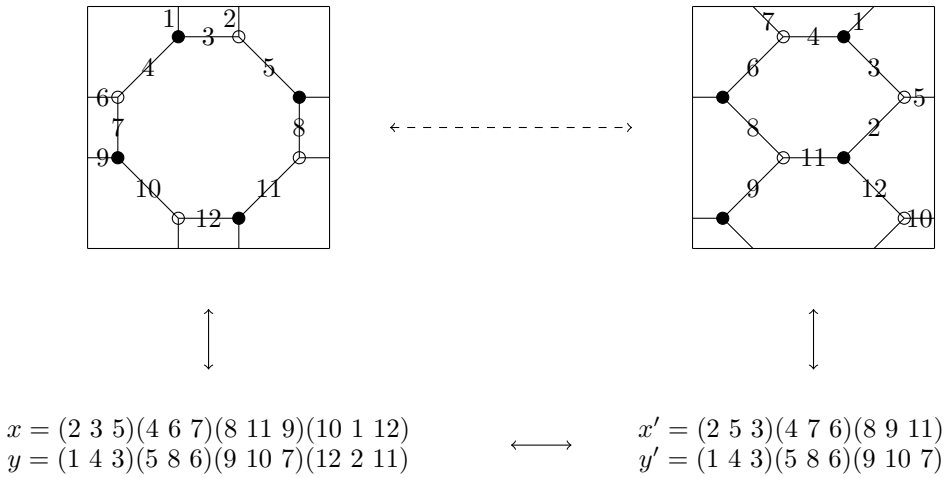

Figure 8: The untwisting procedure for the fat bipartite graph of Fig. 2.

This *untwisting* procedure merely changes the fat structure of the fat bipartite graphs (and it is obviously involutive). The underlying graph stays untouched, but now one has a new embedding of the same graph into another surface (which is such that the faces are topological disks):

$$T^2 \hookleftarrow \Gamma \hookrightarrow \Sigma_\Gamma \ . \tag{31}$$

Let's denote ϵ_{Σ_Γ} the intersection pairing on Σ_Γ. The Poisson bracket on $\mathcal{L}_\Gamma$ in which we're interested is defined as:

$$\{W_{L_1}, W_{L_2}\} = \epsilon_{\Sigma_\Gamma}(L_1, L_2) W_{L_1} W_{L_2} \ . \tag{32}$$

Remark 5. *Link with mirror symmetry? Maybe in an Appendix? Why are we only considering tori ?? Is there a link between super-conformality and integrability??*

Remark 6. *In remark 4 we emphasized the fact that the faces of the bipartite fat graph correspond to the cycles of the permutation xy. In the conjugated surface, these are the cycles of $(x')^{-1}y'$. The latter permutation correspond to the following procedure: starting from any edge, turn maximally right (or, go to the edge directly after it) at its black endpoint, then turn maximally left (or, go to the edge directly before this new edge) at the white endpoint of the new edge, and repeat until one comes back to the original edge. These special paths are called* zig-zag paths. *The zig-zag paths of the original bipartite graph are also correspondingly mapped to the boundary of faces in the one one the conjugated surface: $x^{-1}y = x'y'$.*

2.6 Local definition of the Poisson structure

The Poisson structure defined above using the intersection pairing on the conjugated surface Σ_Γ is, as such, difficult to handle. To actually compute the Poisson bracket of two functions on $\mathcal{L}_\Gamma$, it goes without saying that it would be nice to have a more straightforward way than derive the conjugated surface, and then use its intersection pairing. Luckily, there is a local definition of this Poisson bracket that allows for calculations.

Definition 13. *Let v be a vertex in a graph Γ, and let $\vec{e_1}, ..., \vec{e_n}$ be the edges incident to v oriented in such a way that v is their source. We define the following abelian group at v:*

$$\mathbb{A}_v = \left\{ \sum n_i \vec{e_i} \middle| \sum n_i = 0, n_i \in \mathbb{Z} \right\} \ . \tag{33}$$

It is generated by the $(\vec{e_j} - \vec{e_i})$ for $1 \leq i < j \leq n$.

Proposition 2. *Let Γ be a fat graph, and let v be a vertex of Γ. There is a unique skew-symmetric bilinear form $\delta_v : \mathbb{A}_v \wedge \mathbb{A}_v \to \frac{1}{2}\mathbb{Z}$, such that if the triple $(\vec{e_i}, \vec{e_j}, \vec{e_k})$ is positively oriented, and if $\gamma_l = \vec{e_j} - \vec{e_i}$ and $\gamma_r = \vec{e_k} - \vec{e_i}$, then $\delta_v(\gamma_r \wedge \gamma_l) = \frac{1}{2}$.*

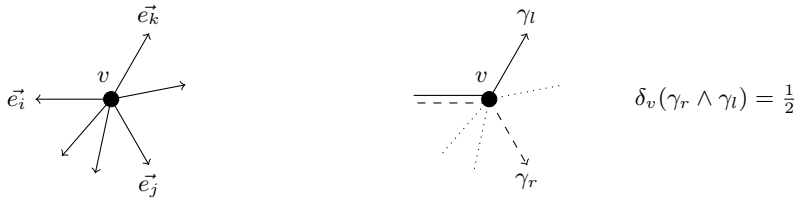

Proof. Let $(x_1, ..., x_m)$ be the cyclically ordered set of endpoints of edges incident to v, and let γ_i be the path $x_i v x_{i+1}$. The γ_1, ..., γ_m generate $\mathbb{A}_v$, and $\sum_i \gamma_i = 0$. Imposing

$$\delta_v(\gamma_i \wedge \gamma_{i+1}) = \frac{1}{2} \tag{34}$$

completely defines δ_v, and since $\sum_i \gamma_i$ is in the kernel of δ_v, the latter is well-defined on $\mathbb{A}_v$. □

Definition 14. *For any L_1 and L_2 two oriented loops on Γ a bipartite fat graph, set*

$$\epsilon(L_1, L_2) = \sum_v \mathrm{sgn}(v)\delta_v(L_1, L_2) \ , \tag{35}$$

where the suns runs over all vertices shared by L_1 and L_2, and where $\mathrm{sgn}(v)$ *is* 1 *(resp. -1) if v is a white (resp. black) vertex.*

Proposition 3. *This ϵ coincides with the intersection pairing on the conjugated surface ϵ_{Σ_Γ}.*

Proof. See the Appendix of [GK13]. □

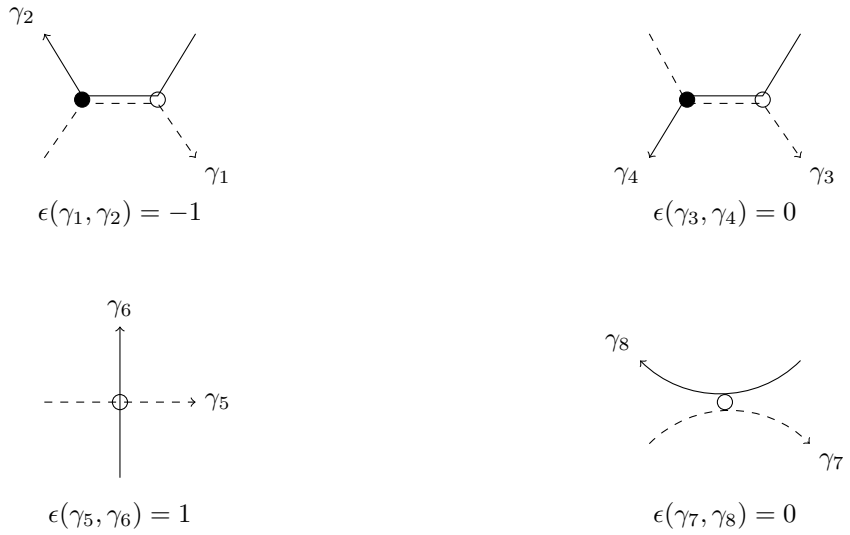

Figure 9: Examples of local contributions to the pairing.

3 Bipartite fat graphs on $\mathbb{T}^2$: cluster structure and integrability

In the following, we restrict to the cases in which the genus of the bipartite fat graph is one, equivalently, in which there is an embedding of a bipartite graph on a real torus T^2 such that the faces are topological disks. Most of the results are known in that case, and not necessarily easy to extend, and moreover, the integrability of the dynamical system we will define relies on Pick's theorem which does not exist in higher dimension (genus), at least in such a nice form.

3.1 The cluster nature of the dimer model

Recall that in Section **??** we have defined the modified partition function corresponding to a bipartite graph embedded in surface such that the faces are topological disks, together with a weight function. Moreover, in Section 2.4, we have shown that bipartite graphs embedded in surfaces in such a way that the faces are topological disks are actually exactly the same thing as bipartite fat graphs, hence in the end we have defined a modified partition function Z_Γ corresponding to any bipartite fat graph Γ, together with a weight function.

Let g be the genus of the fat graph Γ (i.e., the genus of the closed surface Σ it defines). The modified partition function is a Laurent polynomial in $2g$ variables which keep track of the winding around $H_1(\Sigma, \mathbb{Z})$, and the coefficient of this polynomial depend on the weight function w. Actually, the whole point of defining the

modified partition function instead of the simple partition function was that the modified one does not depend on the weight function itself, but merely on its class in $H^1(\Gamma, \mathbb{C}^\times)$.

The degree of a monomial in Z_Γ defines a point in $\mathbb{Z}^{2g}$, and the convex hull of the set of points corresponding to all the monomials in Z_Γ is called the *Newton polyhedron* of Z_Γ.

There is quite a lot freedom in the choice of the $2g$ variables that keep track of the winding - equivalently, there is freedom in the choice of the fundamental domain used to compute Z_Γ. In the end, it translates to the natural action of $\mathbb{Z}^{2g} \rtimes \mathrm{SL}(2g, \mathbb{Z})$ on the lattice $\mathbb{Z}^{2g}$ (the first factor correspond to translations and the second to linear transformations).

Hence a bipartite fat graph defines a class of Newton polyhedra up to $\mathbb{Z}^{2g} \rtimes \mathrm{SL}(2g, \mathbb{Z})$.

Definition 15. *Two bipartite fat graphs are said to be equivalent if they define the same class of Newton polyhedra up to* $\mathbb{Z}^{2g} \rtimes \mathrm{SL}(2g, \mathbb{Z})$.

In each equivalence class of bipartite fat graphs there are *minimal* bipartite fat graphs, which have a minimal number of faces.

Proposition 4. *There exist elementary transformations of the bipartite fat graph, namely the presented-below* spider moves *or* shrinking/adding a 2-valent vertex*, that do not change the equivalence class. Moreover, any two equivalent minimal bipartite fat graphs on a* 2*-torus are related by a sequence of these elementary transformations.*

Proof. This proposition is a consequence of a theorem given in [Thu04]. In this paper, Thurston defines a studies *triple crossing diagrams*, which are unions of isotopy classes of arcs in a disk realizing a matching of n *in* and n *out* points placed on the boundary of the disk. The theorem is that:

1. In a disk with $2n$ such points on the boundary, all $n!$ matchings of *in* endpoints with *out* endpoints are achieved by minimal triple crossing diagrams.
2. Any two minimal triple point diagram with the same matching of the endpoints are related by a sequence of $2 \leftrightarrow 2$ *moves*.

These $2 \leftrightarrow 2$ moves are combinatorial transformations of triple diagrams which becomes spider moves when expressed in the language of bipartite graphs. Let us refer to [GK13] for more details on this. □

A spider move is either the transformation of the bipartite fat graph presented in Fig. 10, or the one with black vertices replaced by white ones, and vice-versa.

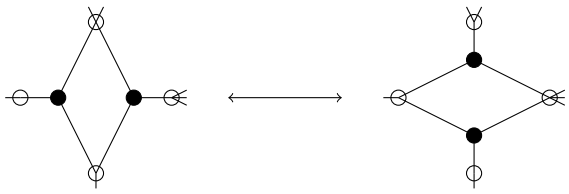

Figure 10: A spider move

On the other, one of the many shrinking/adding a 2-valent vertex moves is described in Fig. 11. There are many of these move because beside exchanging black and white vertices the splitting of the n edges adjacent to a vertex can be done in $\binom{n}{2}$ different ways.

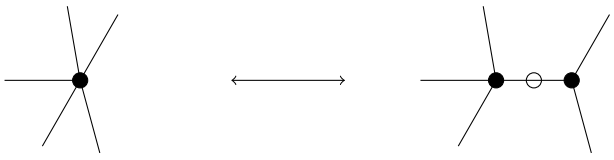

Figure 11: Shrinking/adding a 2-valent vertex

Two bipartite fat graphs related through a sequence of these elementary transformations can be quite different: for example, the two graphs shown in Fig. 12 are equivalent. Starting from the one on the left, doing a spider move at the greyed face and then removing two two-valent vertices yield the bipartite fat graph on the right. Note that the total number of edges is not preserved. As one could check by computing the (modified) partition function of the dimer model, the number of dimer configurations is not preserved either (it is nine one the left, and eight on the right). However, these two bipartite fat graphs define the same class of Newton polygon, as it can, once again, be checked explicitly.

In fact, there is more: for each of these elementary transformation $\Gamma \mapsto \Gamma'$ of bipartite fat graphs, there is a way to map the original face weights (that parametrize $H^1(\Gamma, \mathbb{C}^\times)$) to the face weights of Γ', in such a way that the modified partition function is invariant under this procedure. In the case of adding/removing 2-valent vertex, it is easy: one merely has to leave the face weights as they were. In the case of the spider moves, the transformation of the face weights is more interesting, and is given in Fig. 13.

A face weight transformation as the one shown in Fig. 13 defines a so-called *cluster Poisson birational isomorphism* $i_{\Gamma,\Gamma'} : \mathcal{L}_\Gamma \dashrightarrow \mathcal{L}_{\Gamma'}$, along which *most* of the spaces $\mathcal{L}_\Gamma$ and $\mathcal{L}_{\Gamma'}$ can be identified.

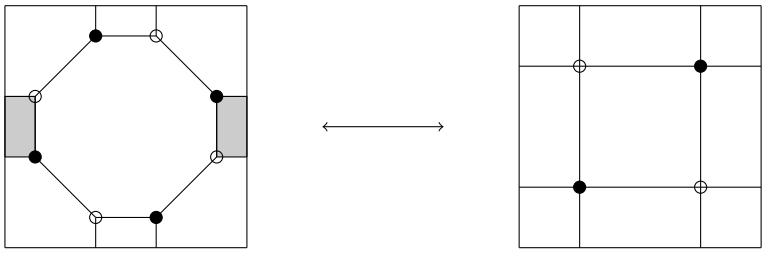

Figure 12: Two graphs related by elementary transformations

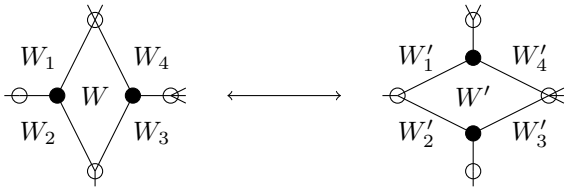

$$\begin{cases} W' &= W^{-1} \\ W_i' &= W_i(1+W) & i=1,3 \\ W_j' &= W_j(1+W^{-1})^{-1} & j=2,4 \end{cases}$$

Figure 13: Distinguished edge weights modifications through a spider move.

Definition 16. *Let Δ be a Newton polyhedral in $\mathbb{Z}^{2g}$, and let $|\Gamma|$ be the equivalence class of all bipartite fat graphs on Σ_g corresponding to Δ. Let $\mathcal{X}_\Delta$ be the space*

$$\mathcal{X}_\Delta = \amalg_{\Gamma\in|\Gamma|}\mathcal{L}_\Gamma/(\sim)\ , \tag{36}$$

where $\sim$ describes the identifications corresponding to the birational isomorphisms coming from the elementary transformations.

The space $\mathcal{X}_\Delta$ has a special structure: it is said to be a cluster $\mathcal{X}$-variety.

Proposition 5. *The Poisson bracket is preserved via the Poisson birational isomorphisms, hence it induces a Poisson bracket on $\mathcal{X}_\Delta$. The Poisson manifold $(\mathcal{X}_\Delta, \{\cdot,\cdot\})$ is the phase space of the dynamical system corresponding to the polyhedron Δ.*

Proof. Proof of the preservation of the Poisson bracket. □

3.2 Casimirs

As introduced in remark 6, a *zig-zag path* on a bipartite fat graph Γ is an oriented path that turns maximally left at each white vertex and maximally right at each black vertex. We also emphasized that such a path on Γ corresponds to a face in the conjugated surface, hence *it is in the kernel of the intersection pairing.*

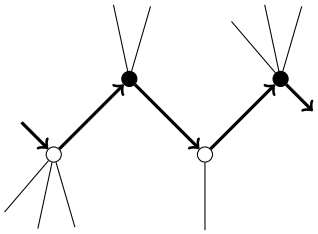

Figure 14: Part of a zig-zag path.

Proposition 6. *If L is a zig-zag loop on a bipartite fat graph then W_L (the monodromy along L) is in the center of the Poisson bracket, meaning that such a function Poisson commute with every other function.*

Proof. Clear from the introduction of this paragraph and the definition of the Poisson bracket in Eq. 32. □

In other words, for a given bipartite graph the W_L are Casimirs of the Poisson bracket on $\mathcal{L}_\Gamma$. There is a relation between them which is $\prod_{\text{ZZL}} W_L = 1$, where the product runs over all the zig-zag loops of Γ.

That this relation exists is merely a translation of the fact each edge appears exactly twice in this product: once for each orientation. See Fig. 15 for an explicit example.

Under the assumption of minimality of $\Gamma \hookrightarrow \Sigma$, it can be proven that the zig-zag loops are not self-intersecting, and that any two distinct lifts of zig-zag paths in the universal cover of Σ intersect at most once. Zig-zag loops are then in $1:1$ correspondence with the elementary boundary segments of the Newton polyhedron Δ. Recall that Δ is drawn in a vector space which is naturally identified with $H_1(\Gamma,\mathbb{R})$. The homologies of the zig-zag loops form the coordinates of the boundary vectors of Δ. Compare for example the homologies of the zig-zag loops given below the graphs in Fig. 15 and the corresponding Newton polygon in Fig. 4.

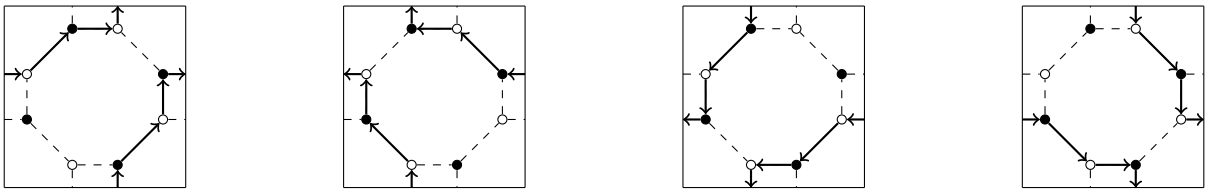

$(1,1)$ $(-1,1)$ $(-1,-1)$ $(1,-1)$

Figure 15: The four zig-zag paths of the bipartite fat graph in Fig. 2.

Remark 7. *The sets of Casimirs of the Poisson brackets on $\mathcal{L}_\Gamma$ for different equivalent Γ glue naturally under the cluster Poisson birational isomorphisms, and give rise to Casimirs on the whole phase space $(\mathcal{X}_\Delta, \{\cdot,\cdot\})$.*

3.3 Hamiltonians and integrability

Recall that the modified partition function of a bipartite fat graph on $\mathbb{T}^2$ (or, which is the same, of its equivalence class modulo elementary transformations) is a Laurent polynomial in two variables. Its coefficients depend on the cohomology class of a weight function on the edges of the graph.

Each monomial in the modified partition function correspond to a point in the corresponding Newton polygon Δ. Points on the boundary of Δ correspond more or less to Casimirs of the Poisson bracket TO EXPLAIN . Coefficients corresponding to points inside Δ are the Hamiltonians of the system.

Let's write it in another equivalent way. The modified partition function can be written

$$Z_{D_0} = \sum_{\mathrm{DC}} \sigma(D) \frac{\mathcal{E}(D)}{\mathcal{E}(D_0)} \ , \tag{37}$$

where the sum runs over all D dimer configurations, and where D_0 is (for now) an arbitrary reference dimer configuration. The ratio of energies of D and D_0 is the monodromy along the 1-chain $D - D_0$, that we are conventionally writing L_{D-D_0}. Hence we can rewrite:

$$Z_{D_0} = \sum_{\mathrm{DC}} \sigma(D) L_{D-D_0} \ . \tag{38}$$

Now that we are dealing with 1-chains (on the graph) instead of dimer configurations, we can assign to each 1-chain its homology class in $H_1(\mathbb{T}^2, \mathbb{Z})$ induced by the embedding $\Gamma \hookrightarrow \mathbb{T}^2$, and decompose:

$$Z_{D_0} = \sum_{a \in H_1(\mathbb{T}^2,\mathbb{Z})} \sigma(a) \tilde{H}_{a,D_0} \ . \tag{39}$$

where $\sigma(a)$ is a sign ± 1, and $\tilde{H}_{a,D_0}$ is the sum of all the L_{D-D_0} for 1-cycles $D - D_0$ whose homology on $\mathbb{T}^2$ is a.

Suppose one has chosen a basis x, y of $H_1(\mathbb{T}^2, \mathbb{Z})$. Then any $a \in H_1(\mathbb{T}^2, \mathbb{Z})$ can be written as a pair (a, b), and Eq. 39 becomes:

$$Z_{D_0} = \sum_{(a,b) \in \mathbb{Z}^2} \sigma(a,b) H_{(a,b),D_0} x^a y^b \ . \tag{40}$$

By definition of the Newton polygon Δ corresponding to this class of bipartite fat graphs, the sum in Eq. 40 is zero outside Δ, hence:

$$Z_{D_0} = \sum_{(a,b) \in \Delta} \sigma(a,b) H_{(a,b),D_0} x^a y^b \ . \tag{41}$$

Proposition 7. *The $H_{(a,b),D_0}$ for $(a,b) \in \mathring{\Delta}$ are the Hamiltonians of the integrable system. There exists a good choice of D_0 such that the Hamiltonians:*

1. *Poisson commute.*
2. *are exactly enough for the dynamical system to be integrable* à la Liouville.
3. *are linearly independent.*

In order to preserve these notes from becoming as long as the original article on the subject, we are going to stay very sketchy in proving this last proposition 7. One can of course always mine [GK13] for more details.

3.3.1 The Hamiltonians Poisson-commute

Let (a_1, b_1) and (a_2, b_2) be two points in the Newton polygon Δ. We want to prove that:

$$\{H_{(a_1,b_1),D_0}, H_{(a_2,b_2),D_0}\} = 0 \ . \tag{42}$$

The Hamiltonian $H_{(a_i,b_i),D_0}$ is the sum of monodromies along the 1-cycles $D - D_0$ that have homology (a_i, b_i). Hence 42 becomes:

$$\left\{ \sum_{D|[D-D_0]=(a_1,b_1)} L_{D-D_0}, \sum_{D|[D-D_0]=(a_2,b_2)} L_{D-D_0} \right\} = 0 \ . \tag{43}$$

The idea of the proof of Eq. 42 is to expand the bracket in Eq. 43 and pair the terms that appear in such a way that each pair is zero. One constructs an involution on the space of dimer configurations of a given homology, such that if $\tilde{D}$ denotes the image of D under this involution, and if D_1 (resp. D_2) has homology (a_1, b_1) (resp. (a_2, b_2)), then:

$$\{L_{D_1-D_0}, L_{D_2-D_0}\} + \left\{L_{\tilde{D}_1-D_0}, L_{\tilde{D}_2-D_0}\right\} = 0 \ . \tag{44}$$

It is clear that if we manage to prove this last fact, then Eq. 42 will hold.

Construction of the involution Let D_1 and D_2 be two dimer configurations on a bipartite graph Γ on a torus. The 1-cycle $D_1 - D_2$ is a disjoint union of:

1. homologically non-trivial loops,
2. homologically trivial loops,
3. edges shared by both dimer configurations D_1 and D_2.

The involution assigns to (D_1, D_2) another pair of dimer configurations, denoted $(\tilde{D}_1, \tilde{D}_2)$ and constructed as follows. For any edge e belonging to a topologically trivial loop of $D_1 - D_2$, one switches the labels: if e belongs to D_1, then one makes it belong to $\tilde{D}_2$ and if it belongs to D_2 then one declares that is also belongs to $\tilde{D}_1$. All other edges keep their labels. It is obvious that this procedure is an involution. Moreover, Eq. 44 holds.

Two easy checks In order to see that Eq. 44 indeed holds, let us use the local definition of the Poisson bracket as in 2.6 in order to write the left-hand side as:

$$\sum_{v \in V(\Gamma)} \mathrm{sgn}(v) \left(\delta_v(D_1 - D_0, D_2 - D_0) + \delta_v(\tilde{D}_1 - D_0, \tilde{D}_2 - D_0) \right) \ . \tag{45}$$

Now, let $\mathcal{V}_1$ (resp. $\mathcal{V}_2$, $\mathcal{V}_3$) be the set of vertices in Γ belonging to a homologically trivial loop (resp. homologically non-trivial loop, shared edge) of the 1-cycle $D_1 - D_2$, and let us split the sum in Eq. 45 into three sums: one on $\mathcal{V}_1$, another on $\mathcal{V}_2$ and the last on $\mathcal{V}_3$.

The point is that the involution we chose implies that the sum:

$$\sum_{v \in \mathcal{V}_1} \mathrm{sgn}(v) \left(\delta_v(D_1 - D_0, D_2 - D_0) + \delta_v(\tilde{D}_1 - D_0, \tilde{D}_2 - D_0) \right) \tag{46}$$

is a sum of zeros, by antisymmetry and the local pairing. Moreover, the sum

$$\sum_{v \in \mathcal{V}_3} \mathrm{sgn}(v) \left(\delta_v(D_1 - D_0, D_2 - D_0) + \delta_v(\tilde{D}_1 - D_0, \tilde{D}_2 - D_0) \right) \tag{47}$$

is also zero since at shared vertices the contributions of the dimer configurations D_1 and D_2 are exactly the same. Hence it remains to prove that

$$\sum_{v \in \mathcal{V}_2} \mathrm{sgn}(v) \left(\delta_v(D_1 - D_0, D_2 - D_0) + \delta_v(\tilde{D}_1 - D_0, \tilde{D}_2 - D_0) \right) \tag{48}$$

is zero, in order to conclude the proof of Eq. 44.

The last step of the proof

Definition 17. *Let $\phi : E \to \mathbb{R}$ be a function on the edges, γ an oriented path on Γ and v a vertex of γ. The bending of ϕ at v is:*

$$b_v(\gamma, \phi) = \sum_{e \in R_v} \phi(e) - \sum_{e \in L_v} \phi(e) \ , \tag{49}$$

where R_v (resp. L_v) denotes the set of edges incident to v which are on the right (resp. left) of γ, as one follows γ in the direction given by its orientation.

Now let X be the set of circular-order-preserving maps from the set of zig-zag paths to $\mathbb{R}/\mathbb{Z}$. Any map $\alpha \in X$ yields a function:

$$\begin{array}{rccc} \phi_\alpha : E(\Gamma) & \to & \mathbb{R} \\ e & \mapsto & \alpha_r - \alpha_l \end{array} \tag{50}$$

where α_r and α_l are the two zig-zag paths passing through the edge e, according to Fig. 16.

Proposition 8. *There is an $\alpha \in X$ such that ϕ_α satisfies, for any simple topologically non-trivial loop γ:*

$$\sum_{v \in \gamma} b_v(\gamma, \phi_\alpha) = 0 \ . \tag{51}$$

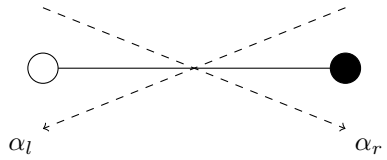

Figure 16: Definition of α_r and α_l

3.3.2 Counting the Hamiltonians

We have seen in Sec. 3.2 that monodromies along zig-zag loops are Casimirs of the Poisson bracket defined on $\mathcal{X}_N$ for some Newton polygon N. The zig-zag loops are in $1:1$ correspondence with the segments on the boundary of N. Hence there are as many independent Casimirs as the number of points on the boundary of N, minus one (since the product of the monodromies along all the zig-zag loops is 1).

One can prove - using the equivalence between minimal triple-crossing diagrams and minimal bipartite graphs on a torus, and results from [Thu04], that the number of faces of a minimal bipartite graph Γ corresponding to a Newton polygon N is twice the area $\mathcal{A}(N)$ of the latter. Hence the dimension of $\mathcal{L}_\Gamma$ is $2\mathcal{A}(N)+1$ (one for every face but one, plus two for the generators of $H_1(\Gamma,\mathbb{Z})$), hence:

$$\dim_{\mathbb{C}} \mathcal{X}_\Delta = 2\mathcal{A}(N)+1 \ . \tag{52}$$

There is a formula known as Pick's theorem, which relates the area $\mathcal{A}(N)$ of a simple convex polygon N with vertices in $\mathbb{Z}^2$ to the number $i(N)$ of its interior lattice points and the number $b(N)$ of its boundary lattice points:

$$2\mathcal{A}(N) = 2i(N)+b(N)-2 \ . \tag{53}$$

From the Eq. 52 and Eq. 53, one deduces that:

$$\dim_{\mathbb{C}} \mathcal{X}_N = 2i(N)+b(N)-1 \ . \tag{54}$$

This implies that there is *enough* Hamiltonians, since once again $e(N)-1$ is the number of independent Casimirs of the Poisson bracket, hence the latter equation expresses that there are as many Hamiltonians as half the dimension of the symplectic sheets of the (holomorphic) Poisson bracket.

Remark 8. *Pick's theorem does not admit a straightforward generalisation to higher dimensions. If one considers that it does, for example as the Ehrhart-Macdonald reciprocity for Ehrhart polynomials, it is surely more difficult and not as generic as in the case of convex polygons.*

3.3.3 Spectral curves and the linear independence of the Hamiltonians

Spectral curve and a compactification from N Any modified partition function Z of a bipartite fat graph on a torus is a Laurent polynomial in variables x and y. Hence the zero locus of Z defines a algebraic curve in $\mathbb{C}^\times\times\mathbb{C}^\times$ called the *spectral curve*. The Newton polygon N of Z yields a *toric compactification* of this spectral curve, in which one adds points at infinity corresponding to the lattice points in the boundary of N, in the following way.

Thanks to the action of $\mathbb{Z}^2\ltimes \mathrm{SL}_2(\mathbb{Z})$ on N, one can always assume that a given side of N lies on the horizontal axis, between the lattice points $(0,0)$ and $(k,0)$, with the rest of N in the upper-half part of the lattice. In the coordinates x,y corresponding to this representation of N, the modified partition function $Z(x,y)$ can be written:

$$Z(x,y) = Z_0(x)+yZ_1(x)+...+y^kZ_k(x) \ , \tag{55}$$

with the Z_i polynomials in x. The *points at infinity* have coordinates $(x_\alpha,0)$ where x_α runs over the roots of the polynomial $Z_0(x)$. Doing this procedure for every face of N indeed compactifies the spectral curve $\{Z=0\}$.

The toric point of view The convex integral polygon N defines a complete projective toric surface $\mathcal{N}$ (possibly singular) together with a T-equivariant line bundle L over $\mathcal{N}$ (see [Ful93] for a general introduction to toric geometry).

The torus $(\mathbb{C}^\times)^2$ acts on $\mathcal{N}$, and there is a unique 2-dimensional orbit which is itself a 2-torus. The complement of it is called the divisor at infinity $\mathcal{N}_\infty$. The shape of the latter is determined by the polygon N: the irreducible components are projective lines corresponding to the edges of $\mathcal{N}$, and intersections match the vertices of $\mathcal{N}$.

Since the toric surface contains the torus $(\mathbb{C}^\times)^2$ as a dense open subspace, it provides a compactification of the spectral curve, which coincides with the one presented in the previous paragraph.

Independence of the Hamiltonians Here even more than before we will stay sketchy to avoid having to give the lengthy technical details needed to properly define and prove the statements that follow. Let us refer to Section 7 of [GK13] for more details.

Laurent polynomials corresponding to the given Newton polygon N define sections of the equivariant line bundle L over $\mathcal{N}$. The idea is that fixing the coefficients of these polynomials corresponding to monomials on

the boundary of N amounts to fix the intersection of the curves defined by the zero locus of the section, with $\mathcal{N}_\infty$. Having done that, one can forget about the divisor at infinity and restrict to a curve in $\mathbb{C}^\times \times \mathbb{C}^\times$.

Changing the coefficient of the monomials corresponding to points in the interior of N does not change the prescribed intersection with $\mathcal{N}_\infty$, and that the corresponding action of the complex vector space generated by the points in the interior of N on the moduli space of curves corresponding to Laurent polynomials with fixed coefficients on the boundary of N is transitive. Since the Hamiltonians are the coefficients of the monomials corresponding to points in the interior of N, their differentials at a point of the moduli space generate the tangent space of the moduli space at this point, hence the Hamiltonians are linearly independent.

3.4 An explicit example

Consider again the bipartite graph Γ on $\mathbb{T}^2$ in Fig. 17, and let us choose a spanning tree $T \subset \Gamma$. Let us use the gauge transformations to set the weight of the edges of the spanning tree to 1. The weights of the edges in $\Gamma \backslash T$ then parametrize $\mathcal{L}_\Gamma$. On Fig. 17 we show the chosen spanning tree with dashed lines, and give names to the weights of the remaining edges.

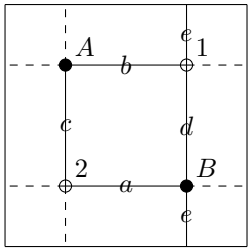

Figure 17: The graph of the explicit example.

Zig-zag loops One can easily see that there are four distinct zig-zag loops on Γ. It is straightforward to compute their monodromy (keeping the convention that edges are oriented from black to white). The result is three independents Casimirs whose expression in terms of a, b, c, d and e reads:

$$C_2 = \frac{b}{d};\ C_3 = \frac{a}{ce};\ C_4 = \frac{ce}{b};\ (C_1 = \frac{d}{a} = \frac{C_4}{C_3 C_2})\ . \tag{56}$$

Partition function and Hamiltonian Let us also compute a (modified) partition function:

$$Z' = (a + \frac{1}{b} + \frac{cd}{b} + \frac{e}{b}) + x + \frac{a}{b}x^{-1} - \frac{ce}{b}y^{-1} - \frac{d}{b}y\ , \tag{57}$$

and using Eq. 56, let us rewrite it in terms of two variables only, say c and e:

$$Z' = (C_3 ce + \frac{1}{C_4 ce} + \frac{c}{C_2} + \frac{C_4}{c}) + x + \frac{C_3}{C_4}x^{-1} - C_4 y^{-1} - \frac{y}{C_2}\ . \tag{58}$$

From Eq. 58 one identifies the (single) Hamiltonian of (a cluster chart of) this integrable system:

$$H = C_3 ce + \frac{1}{C_4 ce} + \frac{c}{C_2} + \frac{C_4}{c} \tag{59}$$

Poisson structure Now we compute the Poisson structure on the phase space. We are especially interested in the Poisson bracket $\{c, e\}$ since c and e are the two variables we have kept in the description we have chosen, and by construction the knowledge of the above mentioned Poisson bracket contains all the possible information about it. To compute $\{c, e\}$ we first choose two loops on Γ whose monodromies are respectively c and e.

Figure 18: Two loops with prescribed monodromies.

The loop on the left of Fig. 18 has monodromy c, hence we call it L_c; the one on the right has monodromy e and is judiciously dubbed L_e. The two loops L_c and L_e have only the two vertices A and 2 in common, hence

$$\epsilon(L_c, L_e) = (-1)\delta_A(L_c, L_e) + (+1)\delta_2(L_c, L_e) \ , \tag{60}$$

where δ_A and δ_2 is the local pairing defined in 2.6, at A and at 2. One finds $\epsilon(L_c, L_e) = -1$, hence for the (coordinate) functions W_{L_c} and W_{L_e} on $\mathcal{L}_\Gamma$:

$$\{W_{L_c}, W_{L_e}\} = -W_{L_c} W_{L_e} \ , \tag{61}$$

an equation one would retrieve by setting $e = \exp(q)$ and $c = \exp(p)$, where q and p are conjugate variables for a canonical (truly canonical, not log-canonical) Poisson bracket $\{q, p\} = 1$. In terms of q and p the Hamiltonian takes the following more comforting form (where now e denotes the exponential):

$$H = C_3 \mathrm{e}^{q+p} + \frac{1}{C_4}\mathrm{e}^{-q-p} + \frac{1}{C_2}\mathrm{e}^{p} + C_4 \mathrm{e}^{-p} \ . \tag{62}$$

4 Concluding remarks

4.1 Two follow-up bounces

4.1.1 A generalisation to other Lie groups

In [FM14], V. Fock and A. Marshakov constructed a broader class of cluster integrable systems, in which the Goncharov-Kenyon setting presented above embeds as a special case. More precisely, let G be a Lie group, $\mathfrak{g}$ its Lie algebra, and $r \in \mathfrak{g} \otimes \mathfrak{g}$ a solution of the classical Yang-Baxter equation:

$$[r_{12}, r_{13}] + [r_{13}, r_{23}] + [r_{12}, r_{23}] = 0 \ . \tag{63}$$

This classical r-matrix r defines a Poisson bracket on G, and this bracket is compatible with the group structure on G, in the sense that the multiplication and the inverse map are Poisson. Moreover, the Ad-invariant functions on G Poisson commute with each other. When G is simple or affine, there is a canonical *Drinfeld-Jimbo* solution to the Yang-Baxter equation.

Fock and Marshakov proved in particular that the Goncharov-Kenyon construction corresponds to the affine case $\hat{A}_n$.

4.1.2 The inverse spectral problem

In [Foc15], V. Fock gives explicit formulae for the *inverse spectral problem*: we have seen that to a point in the phase space - which corresponds to an assignment of numbers in $\mathbb{C}^\times$ to the faces of the bipartite fat graph on T^2, is associated a pair (Σ, L), where S is a compact Riemann surface called *spectral curve*, and where L is a line bundle of degree $g-1$ over Σ. This assignment is an *action-angle* map.

The inverse spectral problem is the following question: given a pair $(\Sigma, \mathcal{L})$ where S is a compact Riemann surface defined by a Laurent polynomial with Newton polygon N, $\mathcal{L} \in \mathrm{Pic}^{g-1}(\Sigma)$ a line bundle of degree $g-1$ over Σ, and a bipartite fat graph Γ with the same Newton polygon N, what is the point $x \in \mathcal{X}_N$ such that the image of this point under the action-angle map is $(\Sigma, \mathcal{L})$?

1. First, one constructs a map d dubbed the *discrete Abel map*, which associates to each face and each vertex of Γ an element of $\mathbb{Z}^Z / H_1(T, \mathbb{Z})$, where Z is the set of zig-zag loops in Γ.
   Since the zig-zag paths on $\Gamma \hookrightarrow \mathbb{T}^2$ correspond to faces on the conjugated surface Σ, and since every face on Σ has a *point at infinity* in its interior, the discrete Abel map in valued in the space of divisors supported at infinity in Σ. Each face is mapped to a principal divisor, each white vertex to a degree-(-1) one, and each black vertex to a degree-$(+1)$ one.
2. Then, one fixes $\mathcal{L} \in \mathrm{Pic}^{g-1}(\Sigma)$ and considers the (infinite dimensional) vector space H of meromorphic sections of $\mathcal{L}$ which are holomorphic away from infinity in Σ (i.e. which can only have poles at the points at infinity in Σ). Let F^i_α be the subspace of H of sections which have order *at least* i at α a point at infinity in Σ. There is an action of $H_1(\mathbb{T}^2, \mathbb{Z})$ on H which preserves the flags. This implies the existence of two maps $\Lambda, M \in H$ such that:
   $$\begin{array}{rccc} \tilde{\Lambda} : & H & \to & H \\ & \psi & \mapsto & \Lambda\psi \end{array} \tag{64}$$
   and an corresponding one with Λ replaced by M, such that $\tilde{\Lambda}(F^i_\alpha) = F^{i+\mathrm{ord}_\alpha(\Lambda)}_\alpha$, and a corresponding statement with Λ replaced by M.
3. Eventually, recall that the Abel-Jacobi map maps white vertices to degree-(-1) divisors at infinity on Σ. Generically (as a condition on $\mathcal{L}$), Riemann-Roch theorem implies that for $d(w)$ such a (-1)-divisor, the space
   $$F^{d(w)} = \bigcap_\alpha F^{d(w)_\alpha}_\alpha \tag{65}$$
   is one-dimensional. There is another (natural) way to assign other one-dimensional vector spaces, this time to black vertices. This assignment comes with maps $V_b \to V_w$ whenever there is an edge between b and w, and these induce a connection on the graph Γ from which it is straightforward to compute the monodromies around faces and $H_1(\mathbb{T}^2, \mathbb{Z})$, hence the corresponding point in the phase space.

There is an explicit formula in terms of values of theta functions on Σ. Let q be a spin structure on Σ, and θ_q the theta function of characteristic q on Σ. Then:

$$x_i = (-1)^{1+l(i)/2} \prod_j \left(\frac{\theta_{q'}(d(j) - d(i))}{\theta_q(t + d(j))} \right)^{\epsilon_{ij}} \tag{66}$$

defines a point $x \in \mathcal{X}_N$ such that $\Sigma(x) = \Sigma$ and $\mathcal{L}(x) = \mathcal{L}$. This is Theorem 1 in [Foc15].

4.2 AdS/CFT correspondence, brane tilings and mirror symmetry

The holographic principle and AdS/CFT correspondence The holographic principle is a supposed property of quantum gravity. It is the idea that the description of a system extending in some space can be encoded in a lower-dimensional boundary of it. One of the main motivation for this idea is Bekenstein -Hawking theory of black holes thermodynamics. Bekenstein observed that the entropy of a black hole is proportional to the area of the horizon, and not the volume inside the horizon. The name comes from an analogy with holograms, in which a 2-dimensional object supports the piece of information needed to reconstruct a 3-dimensional image.

The AdS/CFT correspondence has been motivated by Maldacena in a seminal 1997 paper [Mal99], which is nowadays the most cited paper in high-energy physics with more than 15000 citations at the time of writing. The conjectural correspondence he proposed (and gave a lot of evidence for) relates the supergravity limit of a string theory in $\mathrm{AdS}_5 \times S^5$, and the t'Hooft limit of $\mathcal{N} = 4$ SU(N) super Yang-Mills theory in 4 dimensions. The latter theory has the property of being conformal (hence the name CFT - standing for Conformal Field Theory), meaning that it is symmetric under the *conformal group* in 4 dimensions: $\mathrm{SO}(2, d)$. On the other hand, AdS_5 stands for the *anti-de Sitter* space, a maximally symmetric 5-dimensional Lorentzian (or Riemannian) manifold with constant negative scalar curvature.

The correspondence is still conjectural, because it is very difficult to map explicitly one theory to the other, and also because in its weak form AdS/CFT is merely a map between two different *limits* of these theories, not between the theories themselves. However, there have been many non-trivial checks, such as the fact that some features or quantities - the symmetry group of the theory, the physical correlation functions, or the behaviour under (small) deformations, actually coincide in both theories.

The AdS/CFT correspondence is sometimes called gravity/gauge duality since Yang-Mills theories are the prototypical examples of gauge theories. It is a strong/weak duality in the sense that the strong coupling on one side is equivalent to the weak coupling on the other. This fact is one of the most interesting aspects of the correspondence. In general, it implies that phenomena that are difficult to handle in one of the pictures can be understood much more easily in the other. This very nice behaviour has already been applied to a better understanding of quark–gluon plasmas in QCD (quantum chromodynamics) through the so-called AdS/QCD correspondence, and phenomena such as superconductivity in condensed matter theories through the so-called AdS/CMT correspondence.

More details on the original AdS/CFT correspondence In Maldacena's framework, one considers N coincident $D3$ branes placed in a smooth and topologically-trivial space-time. The branes are massive and thus deform the space-time metric. In order to write explicitly the expression of the latter, let us choose some coordinates (x^μ, r, x^i) on space-time, which correspond to the decomposition:

$$\mathbb{R}^{1,9} = \mathbb{R}^{1,3} \times \mathbb{R}_{\geq 0} \times S^5 \ . \tag{67}$$

The x^μ describe the world-volume of the $D3$'s, $r \in \mathbb{R}_{\geq 0}$ is the coordinate radial to the world-volume of the $D3$'s, and the $x^i \in S^5$ form, together with t, a set of spherical coordinates on $\mathbb{R}^6$. Then, the metric induced by the presence of the branes reads:

$$ds^2 = H^{-1/2}(r)[-dt^2 + d\vec{x}^2] + H^{-1/2}[dr^2 + r^2 ds_{S^5}] \ , \tag{68}$$

with $H(r) = 1 + \frac{L^4}{r^4}$ and where $L^4 = 4\pi g_s N(\alpha')^2$. When $r \to 0$, one speaks of the near-horizon limit. In Maldacena's case, the geometry in the near horizon limit is $\mathrm{AdS}_5 \times S^5$. That is it for the gravity side of the correspondence.

The gauge side is the infrared limit of the world-volume theory of the $D3$'s: each brane carries a U(1)-gauge field, and in the case of N coincident branes the gauge freedom is enhanced to SU(N). There are 32 (scalar) supercharges in type II superstring theories, and the branes break half of them (as explained in [Pol95], since the boundary conditions at the branes exchange the left-moving supercharges with the right-moving ones, hence only half of them are preserved as linear combinations), hence there remains 16 supercharges which correspond to a 4-dimensional theory with 4 supersymmetries, hence the $\mathcal{N} = 4$ SU(N) super Yang-Mills theory.

The Klebanov-Witten model The original AdS/CFT correspondence has been generalized by Klebanov and Witten in [KW98]. The idea is to place N coincident $D3$ branes near a conical singularity, where by conical singularity one means a point (which will correspond to $r = 0$) of a n-dimensional Riemannian manifold X_n at which the metric can locally be written under the form:

$$ds^2 = dr^2 + r^2 g_{ij} dx^i dx^j \ . \tag{69}$$

In Eq. 69, g_ij is a metric on an $n-1$ dimensional manifold X_{n-1}. The conical singularity indeed is singular except in the case where X_{n-1} is a metric sphere. For $n > 2$, the Ricci-flatness of X_n is equivalent to X_{n-1} being an Einstein manifold of positive curvature, as underlined in [KW98].

Klebanov and Witten consider specifically the case $n = 6$, and take the space-time to be $\mathbb{R}^{1,3} \times X_6$, where X_6 is Calabi-Yau, together with N coincident $D3$ branes placed at $\mathbb{R}^{1,3} \times \{r = 0\}$ where $\{r = 0\}$ is the singular point in X_6.

Then Eq. 68 generalizes straightforwardly, as well as the expression of $H(r)$ and L, and the near horizon limit is $AdS_5 \times X_5$. As advertised above, X_5 is an Einstein manifold of positive curvature.

The generalisation of the original AdS/CFT picture is the correspondence between supergravity in $AdS_5 \times X_5$, and the field theory on the world-volume of the $D3$'s at the singularity. In their article, Klebanov and Witten study in detail an example, in which the Calabi-Yau 3-fold is the famous *conifold*, which is the affine variety $C \subset \mathbb{C}^4$ defined by:

$$C = \{z^1 + z^2 + z^3 + z^4 = 0\} \ . \tag{70}$$

The conifold is singular at $\{z_i = 0\}$ and it is a metric cone over a 5-manifold denoted $T^{1,1}$, which is $\mathrm{SU}(2) \times \mathrm{SU}(2)/\mathrm{U}(1)$ where the U(1) factor is the diagonal U(1) subgroup. The correspondence again seems to work, in the sense that there are plenty of non-trivial checks that do not rule out the expected duality between the two theories.

It is difficult, not to be craving for additional examples, and especially nice ones, in which one has a good insight on the two sides of the picture: gauge (world-volume theory) and (super-) gravity.

The spaces $Y^{p,q}$ At the time of writing of [KW98] and during the few following years, only very few 5-dimensional Sasaki-Einstein spaces (a Sasaki-Einstein space is an Einstein metric space whose metric cone is Calabi-Yau) were known explicitly: namely, the round sphere and the space $T^{1,1}$ evoked above. The authors of [GMSW04] solved this issue by introducing an infinite family of Sasaki-Einstein metrics on $S^2 \times S^3$ parametrized by two integers denoted p and q:

$$ds^2_{p,q} = \frac{1-y}{6}(d\theta^2 + \sin^2\theta d\phi^2) + \frac{dy^2}{6p(y)} + \frac{q(y)}{9}(d\psi - cos\theta d\phi)^2 + w(y)[d\alpha + f(y)(d\psi - cos\theta d\phi)]^2 \ , \tag{71}$$

with

$$w(y) = 2\frac{a-y^2}{1-y},\ q(y) = \frac{a-3y^2+2y^3}{a-y^2},\ f(y) = \frac{a-2y+y^2}{6(a-y^2)},\ p(y) = \frac{w(y)q(y)}{6} = \frac{a-3y^2+2y^3}{3(1-y)}, \tag{72}$$

The coordinates live in the ranges:

$$0 \leq \theta \leq \pi,\ 0 \leq \phi \leq 2\pi,\ 0 \leq \psi \leq 2\pi,\ 0 \leq \alpha \leq 2\pi l,\ y_1 \leq y \leq y_2, \tag{73}$$

and the constants appearing are defined by:

$$y_{1,2} = \frac{1}{4p}(2p \mp 3q - \sqrt{4p^2 - 3q^2}),\ l = \frac{q}{3q^2 - 2p^2 + p\sqrt{4p^2-3q^2}},\ a = 3y_1^2 - 2y_1^3 \ . \tag{74}$$

The topological space $S^2 \times S^3$ endowed with the metric defined above and corresponding to the pair of integers (p, q) is denoted $Y^{p,q}$. According to the ideas of [Mal99] and [KW98], all these spaces can be used as the *gravity side* of AdS/CFT dual pairs - at the condition that one is able to decipher the gauge side of the picture, namely understand the world-volume theory of a stack of branes placed at the tip of the singularity of the metric cone over $Y^{p,q}$. This is were toric geometry and brane tilings come in.

The toric case and brane tilings Given a singular Calabi-Yau 3-fold X_6, what is the world-volume theory on N-coincident branes placed at the tip of the singularity $p \in X_6$, i.e. sweeping the volume $\mathbb{R}^{1,3} \times \{p\}$ inside the target space $\mathbb{R}^{1,3} \times X_6$?

By definition, X_6 has holonomy in SU(3), and general arguments shown that the world-volume theory is a $4d$ $\mathcal{N} = 1$ quiver gauge theory, i.e. a gauge theory whose structure is encoded in a quiver (an oriented graph) with potential. Each vertex of the quiver corresponds to a gauge group, and each arrow to a chiral superfield in a bi-fundamental representation. The potential defines a *superpotential* for the theory, and the knowledge of the gauge groups, the chiral superfields and the superpotential completely defines the theory. In the special case where X_6 has holonomy in $\mathrm{SU}(2) \subset \mathrm{SU}(3)$, the supersymmetry of the world-volume theory is enhanced to $\mathcal{N} = 2$.

Some cases are more tractable than a generic choice of X_6: namely, when X_6 is an affine toric Calabi-Yau space. The latter are in one-to-one correspondence with equivalence classes of polygons in $\mathbb{Z}^2$, up to $\mathrm{SL}_2(\mathbb{Z}) \ltimes \mathbb{Z}^2$. In that case, there is a systematic way to built the world-volume theory called *brane tilings methods*. These methods have been developed in a series of papers (see [HV07] and references therein).

[Ken02] [KS04]

Super conformality, isoradial embbedings, toric condition

Maldacena, Klebanov-Witten, more general case of affine Calabi-Yau 3-folds.

Mirror symmetry Interpretation of the torus and the conjugated surface as physical objects in the context of the SYZ mirror picture.

4.3 A conjectural quantization condition through topological strings

References

[Arn89] V. Arnold. *Mathematical methods of classical dynamics*. Springer, 1989.

[Bae18] J. Baez. Geometric quantization. http://math.ucr.edu/home/baez/quantization.html, 2018.

[BFF+78a] F Bayen, M Flato, C Fronsdal, A Lichnerowicz, and D Sternheimer. Deformation theory and quantization. I. Deformations of symplectic structures. *Annals of Physics*, 111(1):61 – 110, 1978.

[BFF+78b] F Bayen, M Flato, C Fronsdal, A Lichnerowicz, and D Sternheimer. Deformation theory and quantization. II. Physical applications. *Annals of Physics*, 111(1):111 – 151, 1978.

[CKTB05] A. Cattaneo, B. Keller, C. Torossian, and A. Bruguières. *Déformation, Quantification, Théorie de Lie*. Société Mathématique de France, 2005.

[FM14] V V Fock and A Marshakov. Loop groups, Clusters, Dimers and Integrable systems. 2014.

[Foc15] V. V. Fock. Inverse spectral problem for GK integrable systems. 2015.

[Ful93] W. Fulton. *Introduction to Toric Varieties*. Annals of mathematics studies. Princeton University Press, 1993.

[GK13] A. Goncharov and R. Kenyon. Dimers and cluster integrable systems. *Annales scientifiques de l'École Normale Supérieure*, Ser. 4, 46(5):747–813, 2013.

[GMSW04] Jerome P. Gauntlett, Dario Martelli, James Sparks, and Daniel Waldram. Sasaki-Einstein metrics on $S^2 \times S^3$. *Advances in Theoretical and Mathematical Physics*, 2004.

[Gro13] Alexandre Grothendieck. Esquisse d'un programme. In *Geometric Galois Actions*, pages 7–48. Cambridge University Press, apr 2013.

[HV07] Amihay Hanany and David Vegh. Quivers, tilings, branes and rhombi. *Journal of High Energy Physics*, 2007(10), 2007.

[JW16] G.A. Jones and J. Wolfart. *Dessins d 'Enfants on Riemann Surfaces*. Springer International Publishing, 2016.

[Ken02] Richard Kenyon. The Laplacian and Dirac operators on critical planar graphs. *Inventiones Mathematicae*, 150(2):409–439, 2002.

[Kon03] Maxim Kontsevich. Deformation Quantization of Poisson Manifolds. *Letters in Mathematical Physics*, 66(3):157–216, 2003.

[KS04] Richard Kenyon and Jean-Marc Schlenker. RHOMBIC EMBEDDINGS OF PLANAR QUAD-GRAPHS. Technical Report 9, 2004.

[KW98] Igor R Klebanov and Edward Witten. Superconformal field theory on threebranes at a Calabi-Yau singularity. *Nuclear Physics B*, 536(1-2):199–218, 1998.

[Mal99] Juan Martin Maldacena. The Large N limit of superconformal field theories and supergravity. *Int. J. Theor. Phys.*, 38:1113–1133, 1999. [Adv. Theor. Math. Phys.2,231(1998)].

[Pol95] Joseph Polchinski. Dirichlet branes and Ramond-Ramond charges. *Physical Review Letters*, 1995.

[Thu04] Dylan P Thurston. From Dominoes to Hexagons. *Arxiv preprint math/0405482*, page 14, 2004.